Penerbit Akademia Baru

Journal of Advanced Research in Applied Mechanics

Journal homepage: www.akademiabaru.com/aram.html
ISSN: 2289-7895

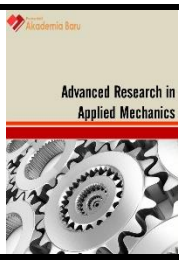

Performance Enhancement of Cold Thermal Energy Storage System using Nanofluid Phase Change Materials

Open Access

Chow Hoong Kee[1], Nor Azwadi Che Sidik[1,*], Siti Nurul Akmal Yusof[1], M'hamed Beriache[2], Ahmad Tajuddin Mohamad[1]

[1] Malaysia – Japan International Institute of Technology (MJIIT), University Teknologi Malaysia, Jalan Sultan Yahya Petra,54100 Kuala Lumpur, Malaysia
[2] Department of Mechanical Engineering, Faculty of Technology, University Hassiba Benbouali, Algeria

ABSTRACT

Cooling Thermal Energy Storage (CTES), for large air conditioning system is becoming paramount in maintaining building comfort, at the expense of huge energy usage. Water based Ethylene Glycol (EG) is used as Heat Transfer Fluid (HTF) with Phase Change Material (PCM) nodule. EG25 of 25% concentration by volume is added into HTF so that the freezing point falls below 0.0° C, and PCM could solidify from liquid to store latent energy. Energy use needed to be prudent and hence, nanofluid CuO was explored for heat transfer enhancement to current CTES system. This paper is to compare the efficiency of heat transfer of energy storage using PCM immersed in EG25 solution and nanofluid CuO. Numerical approach and simulation are conducted to study the improvement of specific heat, latent heat and the behaviour of energy release during melting. The result obtained has proven that nanofluid, EG based mixture is capable of increasing thermal conductivity, enhancing heat transfer. This increases the coefficient of performance and overall efficiency of thermal energy storage.

Keywords:
CTES; phase change materials; nanofluids

1. Introduction

Nowadays, township building is undergoing careful and detailed development by town planner. In the same time, building centralised air conditioning (AC) system such as District Cooling Plant to serve the development of vicinity area has gained much consideration, owe to its economic scale. According to Saidur [1], the AC system is the biggest energy consumer of a building for temperate country like Malaysia, accounting 57% energy usage. Thus, to reduce energy usage, cold thermal energy storage (CTES) is becoming a viable in large centralised AC system, as latent energy storage.

CTES stores latent energy for use at a later time [2-3]. Figure 1 is an illustration of estimated current cooling load demand profile from a typical development in city centre. The latent energy stored during charging at nighttime is released at daytime for use.

* *Corresponding author.*
E-mail address: azwadi@utm.my (Nor Azwadi Che Sidik)

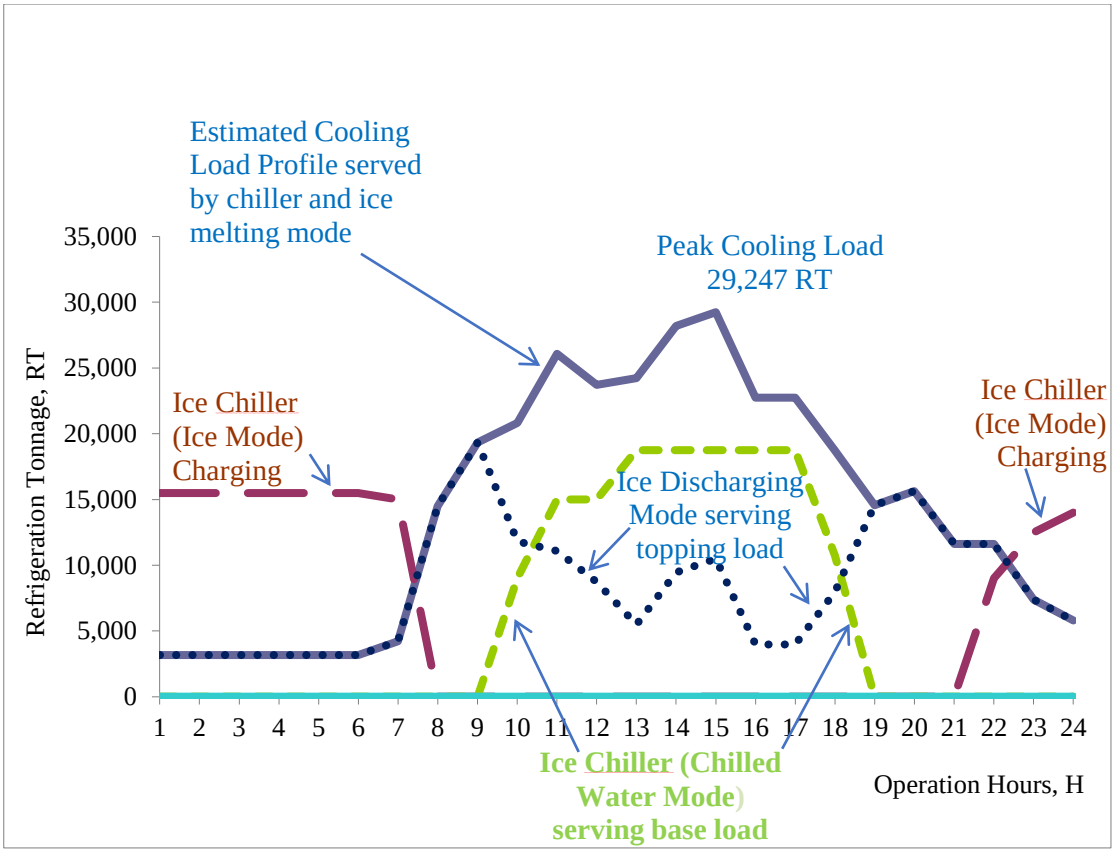

Fig. 1. Estimated cooling load of typical mixed development per day

The common type of CTES are ice on coil and ice ball system. For ice on coil, normally it was described as shell and tube construction, the coil is surrounded by heat transfer fluid (HTF) in a tank [4]. The outer surface of coil is in contact the phase change material (PCM) with cooling energy is transmitted from the coil at freezing point temperature, 0°C during charging/icing and release back to the coil during discharging/melting process. For ice ball system, water and nucleating agent is filled in an encapsulated ball nodule, called ice ball. There is plenty amount of ice balls as PCM and these are loaded in tank, immersed in HTF [5-8]. Recently, there have been few studies on the nanofluid performance CTES [9-15]. Wang *et al.,* [14] found that by using Cu-H20 nanofluid, supercooling degree can be reduced and shorter freezing time was observed during cold storage process. Meanwhile, Ali *et al.,* [15] in their numerical investigation lattice Boltzman method demonstrated that the use of nanoparticles leads to enhancement of thermal conductivity of nano-enhanced phase change materials (PCMs) when compared with conventional PCMs.

The right PCM such as organic [15-18], inorganic [19-20], and eutectic [21] should be selected for particular energy storage applications by considered their thermal properties, physical properties, chemical properties, kinetic properties and economic properties. Organic material such as glycerine and vinyl stearate are divided into paraffin and non-paraffin type, can absorb or release large amount of latent heat due to the nature of the long carbon chain. Having high chemical stability, the paraffin PCM can be used repeatedly and is non-corrosive and non-sub cooling. However, organic PCM has low thermal conductivity [18]. Organic non-paraffin PCM is like paraffin but is relatively corrosive, more expensive and highly flammable [18].

Inorganic PCM is has higher latent heat per unit mass due to higher density [20]. It has higher heat conductivity, approximately 0.5W/m ^{o}C, less flammable, toxicity, corrosive and cheaper compare to organic PCM. Salt hydrate is water based mixed with inorganic salts such as $CaCl_2.6H_2O$. However, the salt hydrate PCM is prone to sub-cooling and phase separation. Zalba *et al.,* [22] has

made classification and cited that suitable PCM is required to fit the requirement of the system as listed in Table 1.

The limitation of conventional PCM is poor heat transfer rate. This is due to their low thermal conductivity and it is impossible to enhance the charging and discharging rate of heat flux. Also, low thermal conductivity would increase the time required for complete melting and solidification processes, decrease the energy storage capacity and yield difficult to retrieve the stored energy. For more than a century time, vast efforts have been done to improve the thermal conductivity of PCMs such as extended surface and fins, microencapsulation, bubble agitation, metal ring and metal matrix insertion, inserting porous media, dispersion of high conductivity particles, etc. This has motivated the present study to conduct a numerical approach and simulation to study the improvement of specific heat, latent heat and the behaviour of energy release during melting. Nanoparticle size contributes greatly to the thermal conductivity enhancement. Few reports have shown that thermal conductivity increase with decrease in nanoparticle size [23-24]. In one of the earliest research, Zeng *et al.,* [25] measured the thermal conductivity enhancement of nanofluid organic phase change material (Ag nanoparticles dispersed in 1-tetradecanol (TD)) and found that the thermal conductivity of the material was enhanced as the volume fraction of nanoparticles increased. Experimental studies by Wu *et al.,* [26] have shown that the total freezing time of Al2O3-H2O nanofluid with SDBS surfactant could be reduced by 20.5% with only 0.2wt.% of Al2O3 nanoparticles. The main goal of this study is to improve the performance enhancement of cold thermal energy storage system using nanofluid phase change materials (NFPCM).

Table 1
Classification of PCM [~~20~~ (22)]]

Phase Change Material		
Organic	Inorganic	Eutectic
Paraffin	Salt hydrate	Organic
Non-paraffin	Metallic	Inorganic-Inorganic
		Inorganic-Organic

2. Methodology

Heat transfer analysis are conducted for melting/discharging of sphere encapsulated PCM. Base HTF, without nanoparticles, and subsequently HTF with nanoparticles by volume fraction of 0.025 and 0.050 with calculated properties are used to beside base HTF to simulate the potential enhancement of heat transfer. Copper Oxide (CuO) will be used as the nanoparticles in the simulation. Transient heat transfer model will be conducted during melting stage of PCM.

3-dimensional model of one sphere encapsulated PCM contained in a metal well insulated tank. Water is used as PCM for the sphere and ethylene glycol of 25% concentration, EG25 is used as the base HTF. The model will focus on the melting/discharging of the ice PCM sphere in transient manner. The potential of heat transfer enhancement here is being analysed.

Hot HTF will flow from inlet, crossing thru the sphere PCM and exit as colder HTF at outlet. During the crossing, the HTF is in contact with the body of the sphere and heat transfer occurred via conduction and convection. The cold energy of PCM is being extracted to chill the hot HTF.

The potential enhancement of melting/discharging for sphere encapsulated PCM is being investigated with the following assumptions:

i. PCM is pure water substance, homogenous and isotropic. No consideration for sub-cooling effect.
ii. PCM is in solid water phase for melting.

iii. No air pocket within the sphere encapsulated PCM to allow for expansion and contraction. Air and vapour phase within sphere are ignored. No buoyancy is assumed.
iv. Initial temperature of PCM is uniform.
v. The outer wall of metal tank is assumed to be fully insulated with no heat transfer across. The metallic component used is aluminium.
vi. The sphere wall capsule is set as aluminium in lieu of blend polyolefins.
vii. The domain is assumed to be large enough for simulation changes take place.
viii. HTF is incompressible.
ix. Inlet mass flowrate of HTF is constant.
x. Inlet temperature of HTF is constant.
xi. The HTF flowrate is accelerated by approximately 25 times to hasten the heat transfer.
xii. The HTF flow is laminar.

2.1 Model Setup

Ansys Fluent 16.0 is chosen as the software to run and simulate the model. The model setup is a simplified version, retaining much of the actual working principle. A sphere encapsulated with PCM is placed at the centre of the steel container as presented in Figure 2. The sphere capsule is set to aluminum as a substitute for the polyolefins material. The metallic tank is also treated to be aluminium with full insulation, adiabatic form and heat loss is negligible. The HTF is moving from the inlet, crossing the sphere of PCM and flowing to outlet.

A sphere encapsulated with PCM is placed at the centre of the steel container. The description setup of sphere capsule is shown in Figure 2(a). Figure 2(b) shows a cut thru at the centre plane for viewing the whole domain. The final condition will focus on the centre-plane as it is assumed to represents overall average result. The domain above consists of 2 parts: HTF filled within metallic container and PCM within cavity of hollow sphere capsule submerged in HTF. The tank is measured by 120 mm x 120 mm x 120 mm while the sphere is set to approximately 97.8 mm external diameter. The thickness of the container wall and sphere skin thickness is set to 1.58 mm.

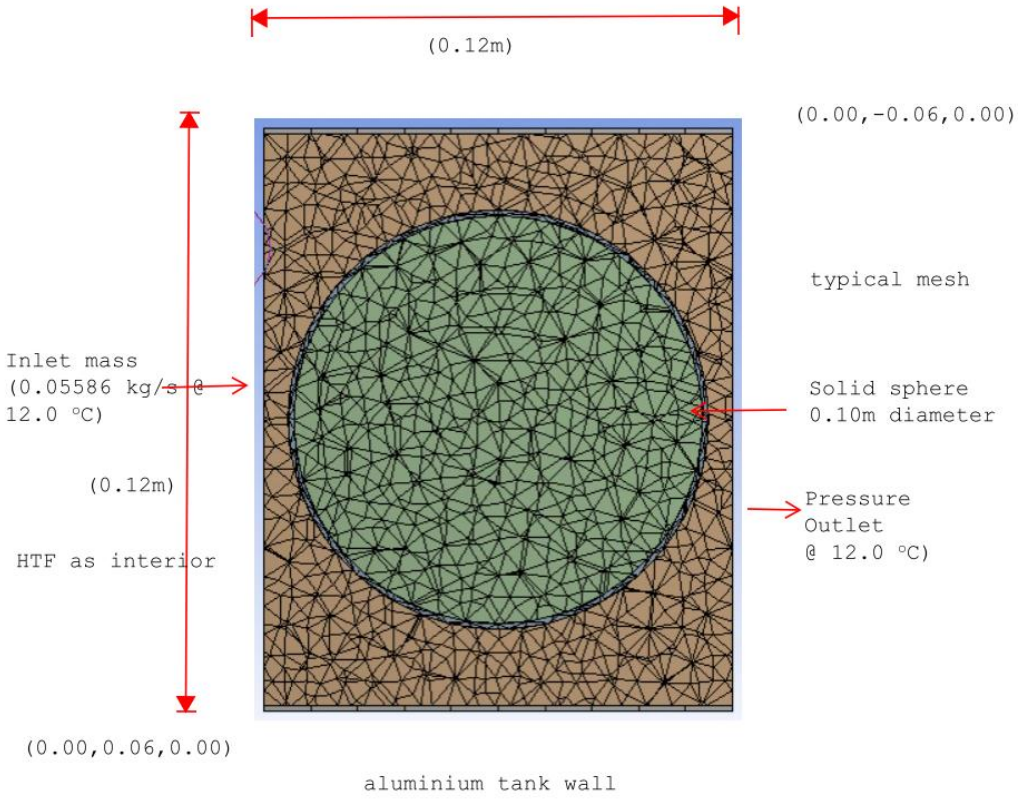

(a) Description of setup

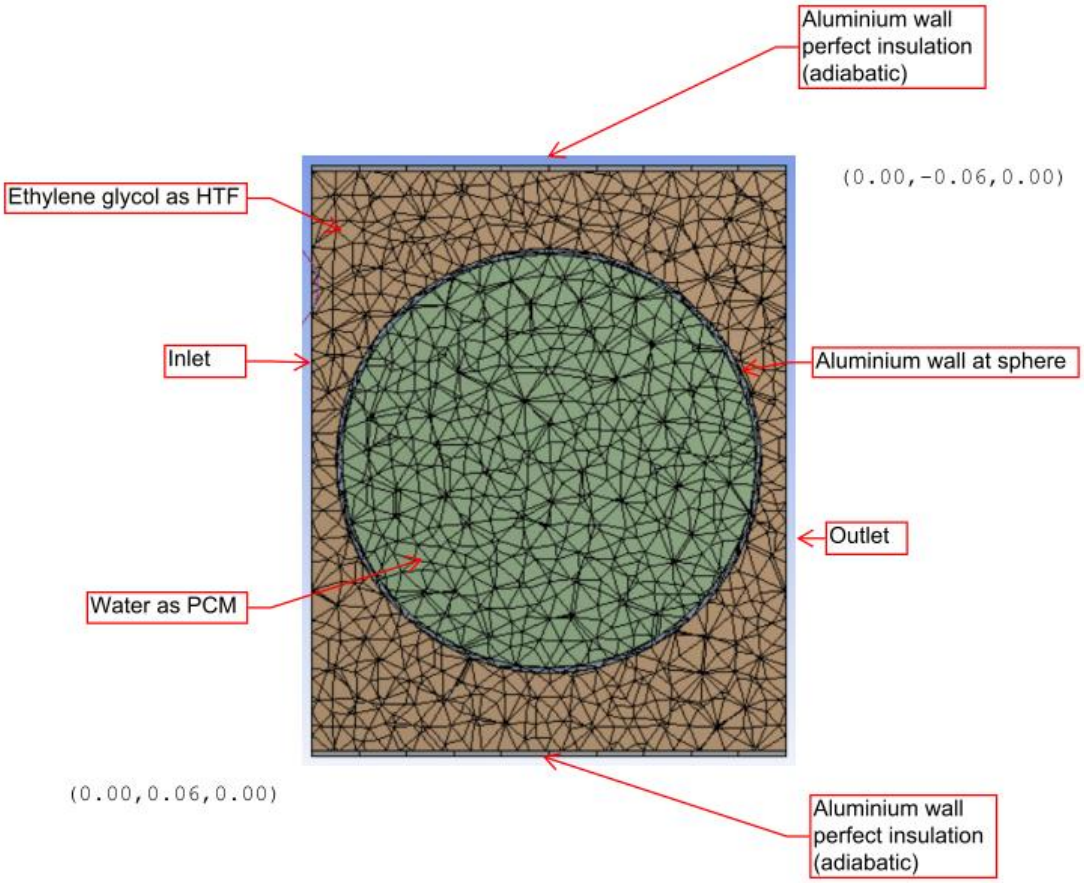

(b) Cut off section view of setup

Fig. 2. A sphere encapsulated with PCM is placed at the centre of the steel container

2.2 Preparation of Mesh

The prepared model from Geometry Modeler is imported into Mesh Design software packaged in Ansys for mesh preparation. Cut cell is utilized to generate complex geometry mesh with reduced time. It consists of mainly hexahedral elements, suitable to align the mesh faces according to curvature. In this manner, the irregularities at gap between the PCM to sphere skin and sphere skin to HTF are reduced and adapted as shown in Figure 3 and Figure 4. This provides regular heat transfer at this interfacing part. Improper meshes at interfaced zone will cause unnecessary computer resources used to solve discontinuities, create improper or divergence result.

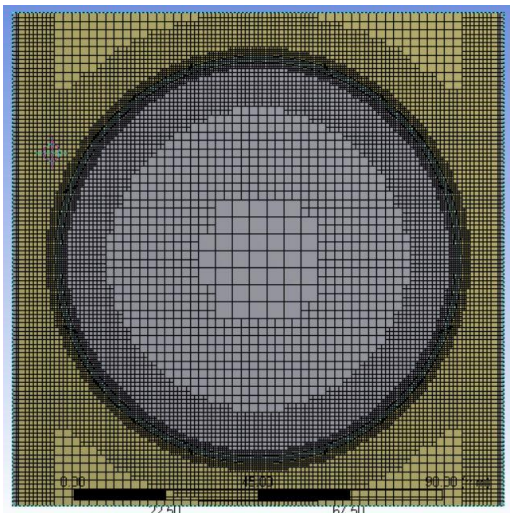

Fig. 3. Cut Cell enhances the curve and boundary

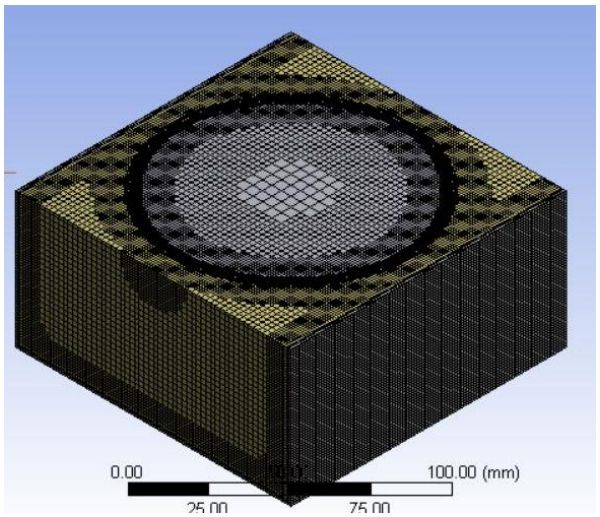

Fig. 4. Cut Cell in Isometric View

2.3 Grid Independent Test

Grid independence test is important to be performed to determine the required size of element to attain correct and acceptable result without compromising further on the computing resources. Too fine mesh will demand much computing while meshes that are too coarse will lead to divergence issue or incorrect result. As the HTF wall and PCM sphere thickness are both set at 1.58mm, the element size at this wall/skin should be lesser than 1.58 mm to capture changes occur within. In this case, 0.82mm mesh element is chosen.

Few coarser grid CFD model produces imprecise result in relative to each other. The finer grid CFD model produces consistent result, starting from nodes quantity of 2719727 to nodes 2924525. The point taken for the grid independent test is at the centre of the outlet plane, with 16.0˚C being the ideal theoretical value upon full release of energy content.

Based on Figure 5, nodes quantity of 2719727 and element size of 2597905 is found to achieve grid independence as shown by the pointed arrow. Hence, nodes quantity of 2854954and element size of 2734272 fine mesh with medium smoothness and 100% relevance parameter provide balance between quality mesh and computing demand. The nodes and elements size in the grid independent test are listed in Table 2.

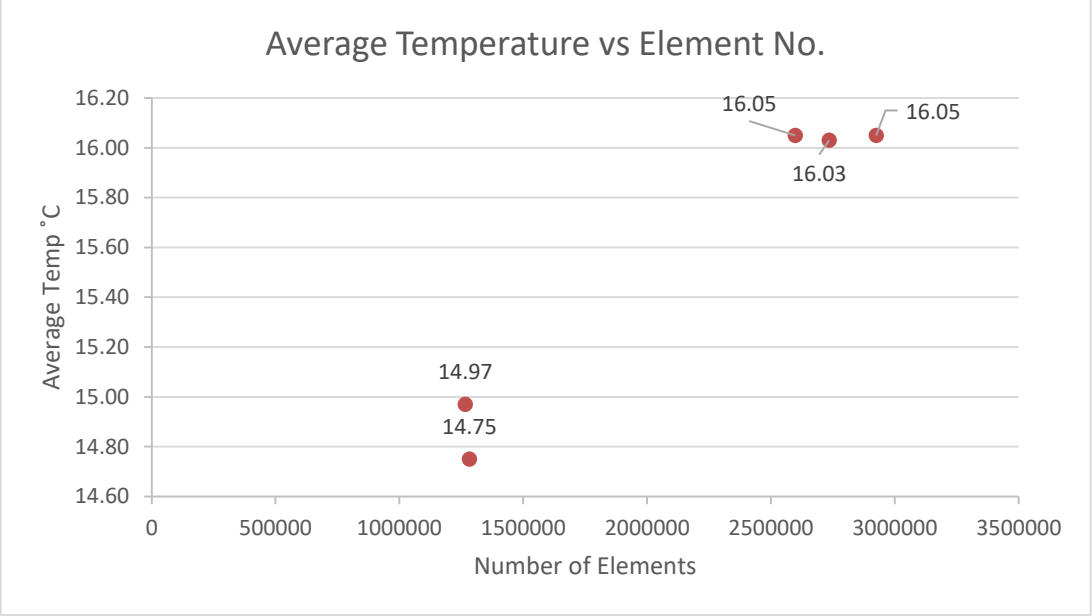

Fig. 5. Graph of independence test

Table 2
The Grid and element mesh for independence test

Item	Wall/Skin Mesh Size	Nodes	Elements	Average Temperature (˚C)
1	0.81	3044571	2924525	16.05
2	0.82	2854954	2734272	16.03
3	0.83	2719727	2597905	16.05
4	0.85	1340069	1282638	14.75
5	0.88	1323837	1265698	14.97

2.3 Fluent Setup

The completed mesh is exported to Ansys Fluent 16.0. In general, 4 core processors are selected for parallel processing to utilize all cores, to accelerate the simulation. Double precision is selected to enhance result accuracy. Next, pressure solver based, transient and gravity inclining to -Y direction is checked. Pressure based solver is suitable as the modeling is using low velocity incompressible fluid and pressure correction is solved using continuity and momentum equation. Transient setting will enable the analysis of heat transfer that varies with time. Gravity is enabled to allow the effect of direction and magnitude gravity onto the flow.

On the model, the energy activated as the focus is on heat transfer. Melting/solidification model is selected, employing on enthalpy-porosity technique, with mushy zone constant 100000 set as default. During melting, the liquid fraction increases from 0 to 1.

The flow nature of the 3 cases is checked using Reynolds Number (Re) formula as

$$\mathrm{Re} = \frac{\rho v D}{\mu} \tag{1}$$

It was found out that the Re is less than 2000, and the flow of HTF is laminar. Further, Laminar is chosen so that turbulence form of equations is not activated, as the flow solution is not critical considering the analysis of end result.

The Nusselt Number (Nu), ratio of convective to conductive heat transfer is given as

$$Nu = \frac{hL}{k} \tag{2}$$

The Stefan Number (Ste) is the ratio of sensible heat to latent heat, given as

$$Ste = \frac{Cp(Th - Tc)}{L} \tag{3}$$

The heat transfer, fluid flow for PCM with nanoparticles in HTF is described by the following conservation equation as described by M. Aurienma *et al.,* [27].

$$\frac{\partial \rho}{\partial t} + \nabla.(\rho \bar{U}) = 0 \tag{4}$$

$$\frac{\partial}{\partial t}(\rho \bar{U}) + \nabla.(\rho \bar{U}\bar{U}) = \nabla.\mathrm{P} + \rho \bar{g} + \nabla.\tau + \dot{F} \tag{5}$$

$$\frac{\partial}{\partial t}(\rho H) + \nabla.(\rho \bar{U} H) = \nabla.(\mathrm{K}\nabla \mathrm{T}) + S \tag{6}$$

The HTF is using ethylene glycol as material with the modified properties as listed in Table 3. The purpose of the properties is to condition the properties like having nanoparticles blended with respective volume fraction in EG as nanofluid.

Table 3
The calculated properties for base and nanofluid

Heat Transfer Fluid and its Constituents	Density, ρ (kg/m3)	Viscosity, μ (Pa-sec)	Cp (J/kgK)	K (W/m-K)	β, (1/K)	L (J/kg)	Pr	Fusion Point (°C)
Solid CuO NanoParticle	6,510.00	0.0000	540.00	18.000	0.000000	0	0.00	0.0
Basefluid with EG25, volfrac = 0.000	1,039.00	0.0042	3,483.50	0.456	0.000610	234,668	32.06	-4.0
Basefluid with EG25, Nanofluid, volfrac = 0.025	1,175.78	0.0045	3,076.06	0.489	0.000526	202,185	28.15	-4.0
Basefluid with EG25, Nanofluid, volfrac = 0.050	1,312.55	0.0048	2,753.54	0.523	0.000459	176,473	25.14	-4.0

From Brinkman [28], the density of the nanofluid is derived from

$$\rho_{nf} = (1 - \emptyset)\rho_f + \emptyset \rho_s, \tag{7}$$

While the viscosity of the nanofluid is determined using

$$\mu_{nf} = \frac{\mu_f}{(1-\emptyset)^{2.5}}, \tag{8}$$

The heat capacities are obtained from

$$\begin{aligned}(\rho c_p)_{nf} &= (1-\emptyset)(\rho c_p)_f + \emptyset(\rho c_p)_s \\ (\rho\beta)_{nf} &= (1-\emptyset)(\rho\beta)_f + \emptyset(\rho\beta)_s,\end{aligned} \tag{9}$$

The effective thermal conductivity of the nanofluid is calculated using

$$k_{eff} = k_{nf,o} + k_d, \tag{10}$$

where the thermal conductivity of the nanofluid is given by Wasp EJ *et al.,* [29] as

$$\frac{k_{nf,o}}{k_f} = \frac{k_s + 2k_f - 2\phi(k_f - k_s)}{k_s + 2k_f + \phi(k_f - k_s)} \tag{11}$$

The latent heat of the nanofluid is evaluated using

$$(\rho L_h)_{nf} = (1-\emptyset)(\rho L_h)_f, \tag{12}$$

The material of ice-water is set for PCM. *f* is the liquid fraction during the phase change, which varies between zero for solid and one for liquid and is provided as below:

$$f = \begin{cases} 0, \text{ if } T < T_s \\ \frac{T-T_s}{T_l-T_s}, \text{ if } T_s < T < T_l \\ 1, \text{ if } T > T_l \end{cases} \tag{13}$$

where respective temperature is ultimately set as
Solidus temperature, T_s = -4.0˚C,
Liquidus temperature, T_l = 0.0˚C

Selecting with differential temperature between solidus and liquidus temperature of less 1.0˚C yields instable result. This is consistent with the findings by Aniruddha Chatterjee [30], citing that temperature different less 3K and below poses instability result. And in real application, the temperature of full charged PCM during initial stage is -4.0˚C.

The density of ice water is different, changing according to temperature. Being liquid at 4.0˚C, it has density of 1000.0 kg/m^3, while in solid, the density reduces to 916.0 kg/m^3. Hence, it is altered using under piecewise-polynomial equation with the following base input.

$$\begin{aligned}\rho_w(P_{atm,}t) &= 2\times10^{-8}.t^5 - 4\times10^{-6}.t^4 + 2\times10^{-4}.t^3 - 9.5\times10^{-3}.t^2 - 5.5\times10^{-3}.t + 1000.4 \text{ (kg/m}^3\text{)} \\ \rho_i(P_{atm,}t) &= -8\times10^{-4}.t^2 - 17.03\times10^{-2}.t + 916.48 \text{ (kg/m}^3\text{)}\end{aligned} \tag{14}$$

The previous equation was adopted from calculation routines by Otero *et al.,* [31]. Similarly, the specific heat of ice and water is 2108.0 J/kg.˚C and 4188.0 J/kg.˚C respectively. And the specific heat change during phase change of solid and liquid water. The same calculation routines by Otero *et al.,* [31] for PCM is taken and keyed into piecewise-polynomial basing the following:

$$C\rho_w(P_{atm,}t) = 4\times10^{-8}.t^6 - 10^{-5}.t^5 + 8\times10^{-4}.t^4 - 14.3\times10^{-3}.t^3 - 36.48\times10^{-2}.t^2 + 6.7732.t + 4253.4 \text{ (J/kg.}^{\circ}\text{C)} \quad (15)$$

$$C\rho_i(P_{atm,}t) = 7.78.t + 2115 \text{ (J/kg.}^{\circ}\text{C)}$$

Cell zone conditions are set with the material as per Table 4 below. The selection of material will be based on the properties fixed as per intent. As WALL and PCMWALL is boundary skin and required for heat transfer across, and aluminium exhibit excellent heat transfer characteristic, the choice is left as default. However, the WALL of the tank is insulated with negligible heat flux across.

Table 4
Cell zone conditions

Part	Material Setting	Description
PCM	Fluid, Ice	Manual select, others remain unchanged
HTF	Fluid, Ethylene Glycol	Manual select, others remain unchanged
WALL	Solid, Aluminium	Set by default, exhibit heat transfer
PCMWALL	Solid, Aluminium	Set by default, no heat transfer

Boundary conditions are defined in the following Table 5. The mass flow rate is calculated from flowrate at the inlet of pipe and the average distributed over plane area of the steel tank in actual condition but have been hastened by approximately 48 times to reduce computation time. Further, this velocity is still within the laminar region.

Setting the outlet to outflow is unsuitable as it assumes full developed flow with zero flux. Pressure outlet is more appropriate as back pressure or reversed flow exists within the tank domain and outlet is restricted to pipe carrier diameter. The wall is set to zero flux, assuming it is fully insulated with negligible heat transfer.

The PCM and HTF are automatically classified as interior by CFD software. Meanwhile, coupled are set by default for the following interfacing parts:

i. HTF and wall,
ii. HTF with PCM sphere skin,
iii. PCM sphere skin with PCM,

Table 5
Boundary condition

Part	Setting	Properties
Inlet	Mass flow inlet	Mass flow rate, $\dot{m}$ = 0.01010kg/s Inlet temperature = 12.0 ˚C
Outlet	Pressure outlet	Backflow temperature = 12.0 ˚C
PCM / HTF	Interior	Set by default
Interfaces	Coupled	Set by default
Walls	Boundary wall	Heat flux is negligible

On the solution solver algorithm, SIMPLEC is selected over SIMPLE due to its robustness and quicker converged solution. SIMPLEC scheme is used to solve the momentum and continuity equation. Coupled is not chosen as this modeling employs segregated solution scheme. PISO advantages shines if the model is highly skewed and with complicated and odd shape. Discretization for other related properties are as followed in Table 6.

Table 6
Solution method condition

Properties	Setting
Gradient	Green-Gauss Node Base
Pressure	PRESTO
Momentum	Second Order Upwind
Turbulent Kinetic Energy	Second Order Upwind
Turbulent Dissipation	Second Order Upwind
Energy	Second Order Upwind
Transient Formulation	Second Order Implicit

Green-Gauss Node Base averaging scheme produces better accuracy for unstructured meshes. PRESTO is used to provide better accuracy via interpolation of pressure gradient compare to second upwind.

Under solutions control all the settings are left unchanged. Solution initialization is done via hybrid mode with 10 iterations rather than standard mode. It is solving Laplace equation to determine pressure and velocity variables under programmed condition. Under this condition, using hybrid mode produces faster convergence result. Meanwhile standard initialization may be used give better controlled environment by putting desired initial value.

The temperature of PCM zone is patched to -4.0˚C so that PCM initial temperature starts at to -4.0˚C before simulation is performed.

3. Results and Discussion

3.1. Preliminary Results

3.1.1 Validation

The computations were performed for three cases. The first case was the base HTF, the second case was HTF with nanoparticles of 0.025 (by volume fraction) and last case was HTF with nanoparticles of 0.050 (by volume fraction).

The Reynolds Number (Re) used was calculated from Eq. (1) with mass flow rate of 0.01010kg/s, diameter of 0.12 m and viscosity of 0.0042kg/m.s. The Re was found to be within 29.5 to 33.5. Laminar model was selected since the value of Re was below than 2000.

The Nusselt number (Nu) obtained from Eq. (2) for this model is in a good agreement and proportionally to the Re. As Re decreases with the increase nanoparticles, the Nu decreases as well. Nu is based on the 21.50 w/m^{2}K, with diameter of 0.12m and thermal conductivity of 0.46W/m.K. Nu for these cases are 5.56 to 2.49, respectively.

Meanwhile, Stefan Number (Ste) was 0.075 for sensible heat to latent heat ratio of PCM was calculated using Eq. (3).

The blue contour indicates solid region is phasing towards lighter blue, green, yellow and finally with red spot during melting are presented in Figure 6. Figure 6(a) is the result of temperature contour for base HTF. Whereas, Figure 6(b) is the result from previous work [32]. As can been seen from figures, the graphical temperature contour results from Figure 6(a) shows in a good agreement with the previous work [32] from Figure 6(b). However, there is only a slight difference for the time duration.

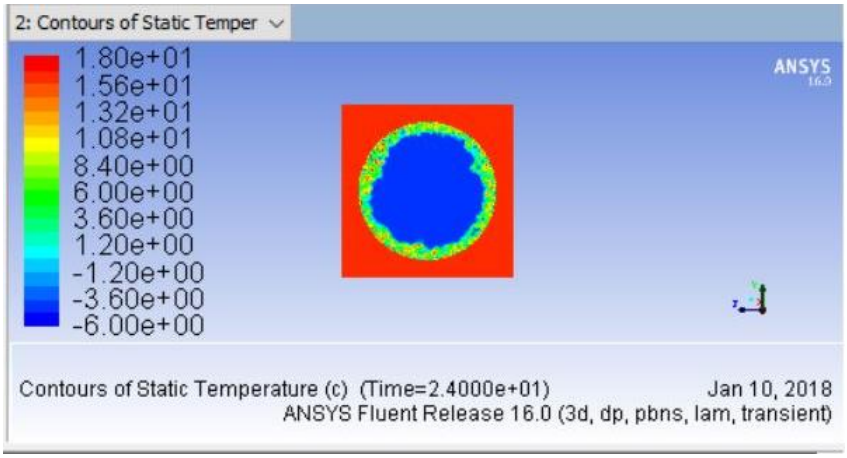

(a) Base HTF: Typical temperature contour, at T=24.0s

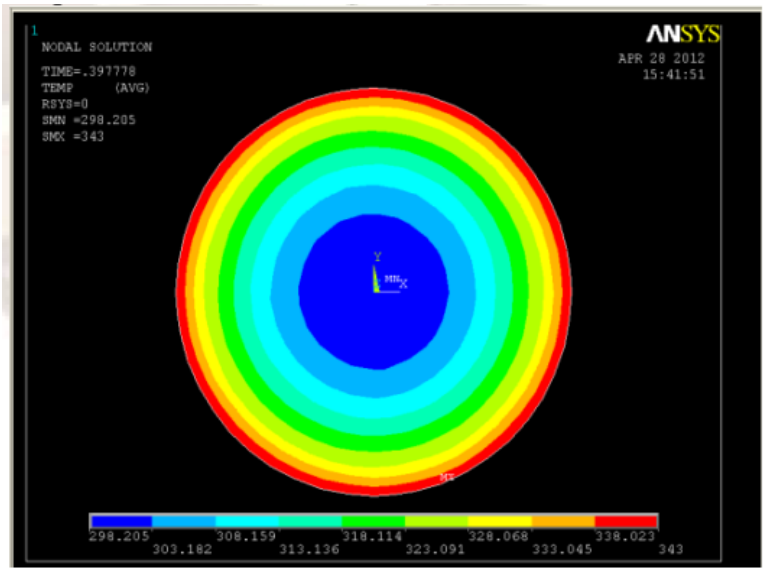

(a) After 0.39 minutes

(b) Temperature contour Paraffin as PCM at T= 23.4s [31]

Fig. 6. Comparison of melt fraction and temperature contour

3.2 *Melting Fraction and Temperature Contour*

Figure 7 shows that at T = 6.0 s, PCM ice starts develops a layer of liquid at the inner interfacing part of sphere, indicated with vague light blue. This is important for nanofluids with volume fractions of 0.025 and 0.050. However, this process is relatively slow, as confirmed by ElGhnam *et al.,* [34], because of the thin layer of fat and therefore, conventional heat transfer is not effective at this time.

At Figure 15, where T = 12.0s, the layer at the sphere inner surrounding become clearer, melting at slightly above temperature of 0.0˚C, forming a liquid ring for both PCM bathed in nanofluid. Now, the main mechanism of heat transfer is influenced convection. The base HTF starts to develop clear ring liquid near the inner sphere surface, while nanofluid HTF shows clearer melt area. Convection mechanism is further enhanced. The HTF with nanoparticles appear to have larger melted layer.

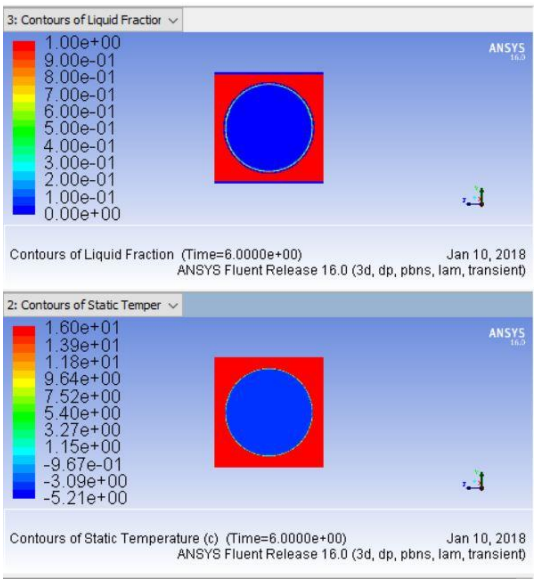

(a) Base HTF

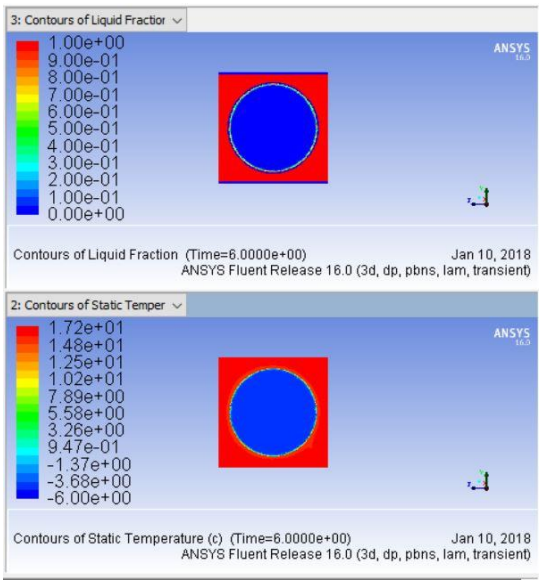

(b) 0.025 by volume fraction of nanoparticles HTF

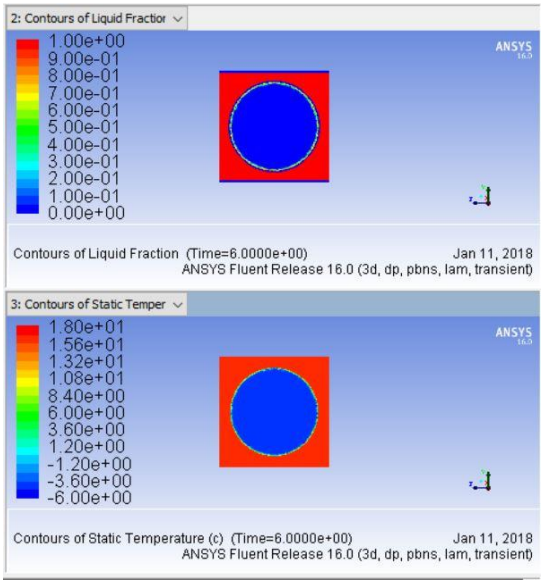

(c) 0.050 by volume fraction of nanoparticles HTF

Fig. 7. Melt fraction and temperature contour at T= 6.0 s

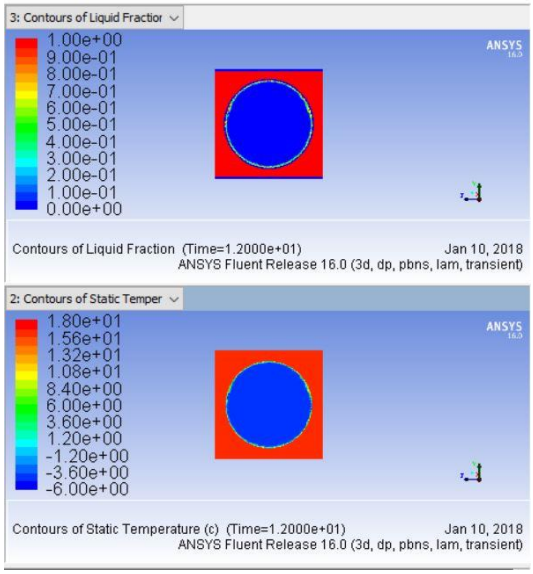

(a) Base HTF

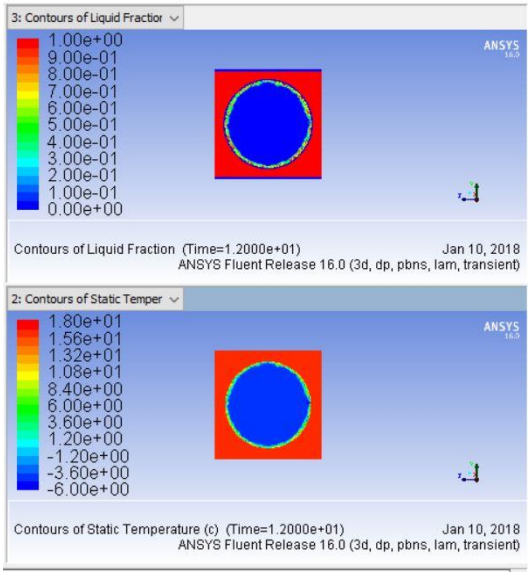

(b) 0.025 by volume fraction of nanoparticles HTF

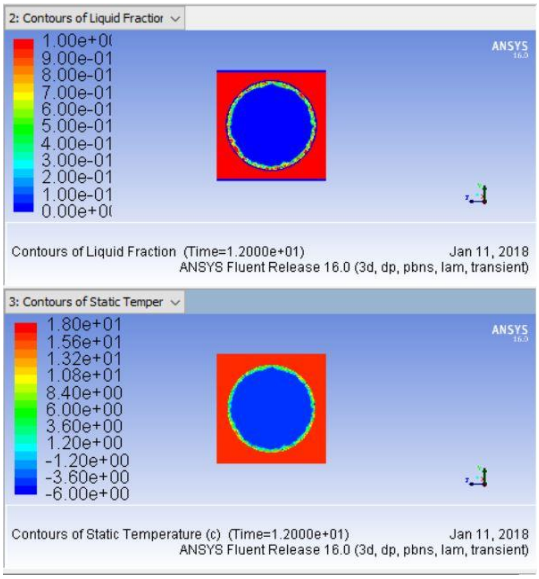

(c) 0.050 by volume fraction of nanoparticles HTF

Fig. 7. Melt fraction and temperature contour at T= 12.0 s

3.3 Heat Transfer Performance

The average enhancement of heat transfer is listed in Table 10. As can be seen from the table, the average enhancement of heat transfer for 0.025 by volume fraction of nanoparticles HTF is 15.45%. While the nanoparticles HTF with 0.050 of volume fraction is 15.29% compared to the base HTF. Based on these results, it can be observed that it is not a significant improvement in the future. At T=30.0s, the improvement is seen significant, with 65.0% and above enhancement over the base HTF. The average melt fraction is 46.0% – 47.0% compared to the base HTF which is only 28%.

One of the limitations is that the increase in nanoparticles has increased the viscosity of the liquid to 0. 0048 Pa.s and therefore the movement of particles is limited to make heat transfer useful. As a result, lower melting fraction is expected. However, these results have a good agreement with the previous work [27].

Item	Time (s)	Liquid Frac (BaseHTF)	Liquid Frac (0.025 VolFrac)	Liquid Frac (0.050 VolFrac)	Enhancement % using 0.025 VolFrac	Enhancement % using 0.050 VolFrac
1	0	0.00	0.00	0.00	0.00	0.00
2	6	0.09	0.11	0.09	25.64	0.24
3	12	0.09	0.12	0.09	30.43	-2.95
4	18	0.17	0.17	0.23	5.02	42.14
5	24	0.26	0.24	0.33	-6.73	25.13
6	30	0.28	0.47	0.46	70.25	65.37
7	36	0.49	0.51	0.51	3.80	4.28
8	42	0.56	0.56	0.57	-0.78	1.66
9	48	0.56	0.63	0.57	11.45	1.79
Average enhancement (%)					15.45	15.29

4. Conclusions

The present study was conducted to evaluate the performance enhancement of cold thermal energy storage system (CTES) using nanofluid phase change materials. Heat transfer analysis is conducted for the melting/discharging of sphere encapsulated PCM. Base HTF, without nanoparticles, and subsequently HTF with nanoparticles by volume fraction of 0.025 and 0.050 was used to simulate the potential enhancement of heat transfer. Copper Oxide (CuO) was used as nanoparticles in the simulation. A transient heat transfer model will be conducted during the melting stage of PCM. One of the more significant findings to emerge from this study is that the thermal conductivity of PCM immersed in the EG25 solution was slightly enhanced by employing the CuO nanoparticle.

However, these findings are limited using the addition of nanoparticles by volume fraction of 0.025 and 0.05 only. Therefore, it is important to consider for determining the appropriate concentration to enhance the performance of CTES. Further research is needed to account for the varying nanoparticle concentration in order to control the charging and discharging of PCM energy.

Acknowledgement

This research was funded by a grant from Ministry of Higher Education of Malaysia (FRGS Grant R.J130000.7824.4X172).

References

[1] Saidur, Rahman. "Energy consumption, energy savings, and emission analysis in Malaysian office buildings." *Energy policy* 37, no. 10 (2009): 4104-4113.
[2] Brian Silvetti, P. E. (2002). Application fundamentals of ice-based thermal storage. *Ashrae Journal*, 31.
[3] Rismanchi, Behzad, Rahman Saidur, Haji Hassan Masjuki, and Teuku Meurah Indra Mahlia. "Cost-benefit analysis of using cold thermal energy storage systems in building applications." *Energy Procedia* 14 (2012): 493-498.
[4] Stovall, Therese K. *CALMAC ice storage test report*. No. ORNL/TM-11582. Oak Ridge National Lab., TN (United States), 1991.
[5] Farid, Mohammed M., Amar M. Khudhair, Siddique Ali K. Razack, and Said Al-Hallaj. "A review on phase change energy storage: materials and applications." *Energy conversion and management* 45, no. 9-10 (2004): 1597-1615.
[6] Dincer, I., and M. A. Rosen. (2002). "Thermal Energy Storage (TES)." *Thermal Energy Storage: Systems and Applications*, Page 93.
[7] Eastman, Jeffrey A., S. U. S. Choi, Sheng Li, W. Yu, and L. J. Thompson. "Anomalously increased effective thermal conductivities of ethylene glycol-based nanofluids containing copper nanoparticles." *Applied physics letters* 78, no. 6 (2001): 718-720.
[8] Wang, Xinwei, Xianfan Xu, and Stephen US Choi. "Thermal conductivity of nanoparticle-fluid mixture." *Journal of thermophysics and heat transfer* 13, no. 4 (1999): 474-480.

[9] Qunzhi, Zhao, Zhang Xuelai, Liang Xiaoyang, Liu Tiantian, and Luo Xiaoxue. "Supercooling and cold energy storage characteristics of nano-media in ball-packed porous structures." *AIP Advances* 5, no. 4 (2015): 041329.
[10] Rahman, Muhammad Mustafizur. "Heat transfer in completely and partially filled spherical phase change thermal energy storage modules." In *AIP Conference Proceedings*, vol. 1754, no. 1, p. 020001. AIP Publishing LLC, 2016.
[11] He, Qinbo, Shuangfeng Wang, Mingwei Tong, and Yudong Liu. "Experimental study on thermophysical properties of nanofluids as phase-change material (PCM) in low temperature cool storage." *Energy conversion and management* 64 (2012): 199-205.
[12] Zhang, Nan, Yanping Yuan, Yanxia Du, Xiaoling Cao, and Yaguang Yuan. "Preparation and properties of palmitic-stearic acid eutectic mixture/expanded graphite composite as phase change material for energy storage." *Energy* 78 (2014): 950-956.
[13] Teng, Tun-Ping. "Thermal conductivity and phase-change properties of aqueous alumina nanofluid." *Energy conversion and management* 67 (2013): 369-375.
[14] Wang, X. J., X. F. Li, Y. H. Xu, and D. S. Zhu. "Thermal energy storage characteristics of Cu–H2O nanofluids." *Energy* 78 (2014): 212-217.
[15] Ryglowski, Brian K., Randall D. Pollak, and Young W. Kwon. "Characterizing the stability of carbon nanotube enhanced water as a heat transfer nanofluid." In *ASME 2010 Pressure Vessels and Piping Division/K-PVP Conference*, pp. 221-230. American Society of Mechanical Engineers Digital Collection, 2010.
[16] Kumaresan, Vellaisamy, Ramalingam Velraj, and Sarit K. Das. "The effect of carbon nanotubes in enhancing the thermal transport properties of PCM during solidification." *Heat and Mass Transfer* 48, no. 8 (2012): 1345-1355.
[17] He, Qin Bo, Shequan Zeng, Shaoyou Yin, and Shuang Feng Wang. "Experimental investigation on nucleation supercooling degree of TiO2–H2O nanofluids for cool storage." *Advanced Materials Research* 550 (2012): 2723-2727.
[18] Aluyor, Emmanuel O., and Mudiakeoghene Ori-Jesu. "Biodegradation of mineral oils–A review." *African Journal of Biotechnology* 8, no. 6 (2009).
[19] Mohamad, Ahmad Tajuddin, N. A. Che Sidik, and B. M'hamed. "Thermo physical enhancement of advanced nano-composite phase change material." *Journal of Advanced Research Applied Mechanics* 54, no. 1 (2019): 1-8.
[20] Wahid, Mazlan Abdul, Seyed Ehsan Hosseini, Hasanen M. Hussen, Hussein J. Akeiber, Safaa N. Saud, and Abdulrahman Th Mohammad. "An overview of phase change materials for construction architecture thermal management in hot and dry climate region." *Applied Thermal Engineering* 112 (2017): 1240-1259.
[21] Raj, V. Antony Aroul, and R. Velraj. "Review on free cooling of buildings using phase change materials." *Renewable and Sustainable Energy Reviews* 14, no. 9 (2010): 2819-2829.
[22] Zalba, Belen, Jose Ma Marın, Luisa F. Cabeza, and Harald Mehling. "Review on thermal energy storage with phase change: materials, heat transfer analysis and applications." *Applied thermal engineering* 23, no. 3 (2003): 251-283.
[23] Angayarkanni, S. A., and John Philip. "Review on thermal properties of nanofluids: Recent developments." *Advances in colloid and interface science* 225 (2015): 146-176.
[24] Tawfik, Mohamed M. "Experimental studies of nanofluid thermal conductivity enhancement and applications: A review." *Renewable and Sustainable Energy Reviews* 75 (2017): 1239-1253.
[25] Zeng, J. L., L. X. Sun, F. Xu, Z. C. Tan, Z. H. Zhang, J. Zhang, and T. Zhang. "Study of a PCM based energy storage system containing Ag nanoparticles." *Journal of Thermal Analysis and Calorimetry* 87, no. 2 (2007): 371-375.
[26] Wu, Shuying, Dongsheng Zhu, Xinfang Li, Hua Li, and Junxi Lei. "Thermal energy storage behavior of Al2O3–H2O nanofluids." *Thermochimica Acta* 483, no. 1-2 (2009): 73-77.
[27] M. Auriemma, and A. Iazzetta. " Numerical Analysis of Melting of Parrafin Wac with Al2O3, ZnOand CuO Nanoparticles in Rectangular Enclosure." *Indian Journal of Science and Technology* 9, no. 3 (2016): 1-8.
[28] Brinkman, H. C. "The viscosity of concentrated suspensions and solutions." *The Journal of Chemical Physics* 20, no. 4 (1952): 571-571.
[29] Wasp, Edward J., John P. Kenny, and Ramesh L. Gandhi. "Solid--liquid flow: slurry pipeline transportation. [Pumps, valves, mechanical equipment, economics]." *Ser. Bulk Mater. Handl. ;(United States)* 1, no. 4 (1977).
[30] Chatterjee, Aniruddha. "Physical and computational models of Marangoni and buoyancy flow during dissolution." PhD diss., University of British Columbia, 2012.
[31] Otero, Laura, Antonio D. Molina-García, and Pedro D. Sanz. "Some interrelated thermophysical properties of liquid water and ice. I. A user-friendly modeling review for food high-pressure processing." *Critical reviews in food science and nutrition* 42, no. 4 (2002): 339-352.
[32] Maheswari, C. Uma, and R. Meenakshi Reddy. "Thermal Analysis of Thermal Energy Storage Systemwith Phase Change Material." *International Journal of Engineering Research and Applications* 3, no. 4 (2013): 617 – 622.
[33] Santim, Christiano Garcia Da Silva, and Luiz Fernando Milanez. "Numerical study of ice melting inside a rectangular cavity and a horizontal cylinder including natural convection." *Int. Rev. Mech. Eng.* 7, no. 5 (2013).

[34] ElGhnam, Reda I., Ramdan A. Abdelaziz, Mohamed H. Sakr, and Hany E. Abdelrhman. "An experimental study of freezing and melting of water inside spherical capsules used in thermal energy storage systems." *Ain Shams Engineering Journal* 3, no. 1 (2012): 33-48.